Biophysical Controls on Carbon and Water Vapor Fluxes across a Grassland Climatic Gradient in the United States

Pradeep Wagle[1*], Xiangming Xiao[1,2], Russell L. Scott[3], Thomas E. Kolb[4], David R. Cook[5], Nathaniel Brunsell[6], Dennis D. Baldocchi[7], Jeffrey Basara[8], Roser Matamala[9], Yuting Zhou[1], and Rajen Bajgain[1]

[1]Department of Microbiology and Plant Biology, Center for Spatial Analysis, University of Oklahoma, Norman, OK 73019, USA

[2]Institute of Biodiversity Science, Fudan University, Shanghai, 200433, China

[3]USDA-ARS, Southwest Watershed Research Center, Tucson, AZ 85719, USA

[4]School of Forestry, Northern Arizona University, Flagstaff, AZ 86011, USA

[5]Environmental Research Division, Argonne National Laboratory, Argonne, IL 60439, USA

[6]Department of Geography - Atmospheric Sciences Program, University of Kansas, Lawrence, KS 66045, USA

[7]Department of Environmental Science, Policy, & Management, University of California Berkeley, Berkeley, CA 94720, USA

[8]School of Meteorology and Oklahoma Climatological Survey, University of Oklahoma, Norman, OK 73019, USA

[9]Biosciences Division, Argonne National Laboratory, Argonne, IL 60439, USA

*Corresponding Author: Email: pradeep.wagle@ou.edu; Tel: 405-325-5568; Fax: 405-325-1595

ABSTRACT

Understanding of the underlying causes of spatial variation in exchange of carbon and water vapor fluxes between grasslands and the atmosphere is crucial for accurate estimates of regional and global carbon and water budgets, and for predicting the impact of climate change on biosphere-atmosphere feedbacks of grasslands. We used ground-based eddy flux and meteorological data, and the Moderate Resolution Imaging Spectroradiometer (MODIS) enhanced vegetation index (EVI) from 12 grasslands across the United States to examine the spatial variability in carbon and water vapor fluxes and to evaluate the biophysical controls on the spatial patterns of fluxes. Precipitation was strongly associated with spatial and temporal variability in carbon and water vapor fluxes and vegetation productivity. Grasslands with annual average precipitation < 600 mm generally had neutral annual carbon balance or emitted small amount of carbon to the atmosphere. Despite strong coupling between gross primary production (GPP) and evapotranspiration (ET) across study sites, GPP showed larger spatial variation than ET, and EVI had a greater effect on GPP than on ET. Consequently, large spatial variation in ecosystem water use efficiency (EWUE = annual GPP/ET; varying from 0.67 ± 0.55 to 2.52 ± 0.52 g C mm^{-1} ET) was observed. Greater reduction in GPP than ET at high air temperature and vapor pressure deficit caused a reduction in EWUE in dry years, indicating a response which is opposite than what has been reported for forests. Our results show that spatial and temporal variations in ecosystem carbon uptake, ET, and water use efficiency of grasslands were strongly associated with canopy greenness and coverage, as indicated by EVI.

Keywords: Ecosystem water use efficiency; Eddy covariance; Enhanced vegetation index, Evapotranspiration; Grasslands; Gross primary production

1. Introduction

In the past two decades, eddy covariance systems have been established in several grassland sites in the United States (U.S.) for investigations of processes controlling carbon and water vapor fluxes, and site specific results have been reported (Baldocchi et al., 2004; Fischer et al., 2012; Krishnan et al., 2012; Ma et al., 2007; Scott et al., 2010; Suyker et al., 2003). However, these observation networks cover only a small portion of grasslands. Sole reliance on individual sites may lead to biased estimates of fluxes at large scales (Biondini et al., 1991; Rahman et al., 2001). The broad distribution of grasslands across contrasting climate and management gradients adds to the complexity of measuring and modeling of fluxes, and understanding the vulnerability of ecosystems to environmental change. It is commonly accepted that ecosystem responses to changes in climatic-forcing variables such as precipitation, temperature, and CO_2 concentration are nonlinear (Burkett et al., 2005; Gill et al., 2002). Grasslands are considered ideal for rainfall manipulation studies because they are highly responsive to interannual variability in precipitation (Knapp et al., 2002). However, precipitation manipulation experiments at individual sites rarely capture this nonlinearity as they tend to have few (only two or three) treatments different from the control and do not manipulate temperature, which can co-vary with precipitation. Flux tower sites now allow comparative analysis, synthesis, modeling, and upscaling of site-level flux measurements (Falge et al., 2002; Gilmanov et al., 2010; Gilmanov et al., 2003; Turner et al., 2003; Xiao et al., 2014). Synthesis of flux data from multiple sites across a climatic gradient allows analysis of the influences of a wider range environmental condition compared with manipulative studies at a single site. Several studies have investigated spatial variability of carbon fluxes (Churkina et al., 2005; Gilmanov et al., 2005; Kato and Tang, 2008; Law et al., 2002; Soussana et al., 2007; Yu et al., 2013; Yuan et al., 2009). These studies have shown that

spatial variability of carbon fluxes is significantly correlated with mean annual temperature (MAT) and precipitation (MAP). However, most of the synthesis studies assembled all biomes together, which masked differences in response over spatial gradients within a biome type, such as grasslands. Compared to carbon fluxes, spatial variability in water vapor fluxes and water use efficiency at the ecosystem level, and the mechanistic understanding of the underlying controlling mechanisms in grasslands is still unclear. In addition, very little is known regarding the relative sensitivity of different grassland communities (C_4, mixed C_3/C_4, and C_3 dominant) across broadly-distributed grasslands to climate. High frequency eddy covariance measurements allow calculation of net ecosystem CO_2 exchange (NEE), evapotranspiration (ET), gross primary production (GPP), ecosystem respiration (ER), and synthetic metrics such as ecosystem water use efficiency (EWUE, which reflects the tradeoff between water loss and carbon uptake in carbon assimilation process), thereby facilitating investigation of responses of carbon and water vapor fluxes to environmental drivers (Huxman et al., 2004; Law et al., 2002).

Satellite remote sensing provides a feasible approach for monitoring vegetation dynamics at ecosystem to global scales (Myneni et al., 1997; Zhang et al., 2003). A better understanding of phenological patterns of vegetation and their drivers is essential to improve climate and biogeochemical cycle models and also to better simulate the exchange of carbon and water vapor fluxes between land surface and the atmosphere (Running and Hunt, 1993). Previously, phenological dynamics have been shown to play a vital role in the variability of carbon and water vapor fluxes at the ecosystem scale for a broad range of ecosystems (DeForest et al., 2006; Hutyra et al., 2007; Ma et al., 2013; Richardson et al., 2010; Wagle et al., 2015). However, the major drivers of spatial variability of phenological metrics and the role of phenological dynamics on spatial variability of fluxes have not been specifically examined for broadly-distributed

grasslands in the U.S. This greatly hampers our understanding of the impacts of future climate change on phenological dynamics and the carbon and water budgets of U.S. grasslands. Further, an establishment of a robust relationship between tower fluxes and remotely sensed data can facilitate extrapolation of site-level fluxes to obtain regional estimates of carbon and water budgets across complex landscapes (Gilmanov et al., 2005; Xiao et al., 2008).

This study covers 12 AmeriFlux grassland sites that represent the distribution of grasslands within the conterminous U.S., including C_4 dominated semi-arid shortgrass prairie of the Southwest (AZ), C_3 dominated Mediterranean grassland (CA), C_3/C_4 mixed temperate grassland of the Northwest (MT) and Southeast (MS), C_4 dominated temperate continental tallgrass prairie of the Midwest (IL, KS) and South Central (OK), and C_3/C_4 mixed humid continental grassland of the Midwest (SD). The objectives of this study were: 1) to analyze the spatial variability in grassland carbon and water vapor fluxes, 2) examine whether a satellite measurement of green biomass (as quantified by the Moderate Resolution Imaging Spectroradiometer (MODIS) enhanced vegetation index, EVI) captures the observed spatial variability in carbon and water vapor fluxes, and 3) determine the responses of GPP and ET to major climatic variables. The time series measurements quantify the conditional statistics associated with seasonal changes in climatic variables and the results provide important insights about predicting the impact of climate change on biosphere-atmosphere feedbacks of grasslands under current and future climatic conditions.

2. Materials and methods

2.1. Site descriptions

The 12 grassland sites used in this study (Fig. S1) cover a broad range of geographic location, grassland type (warm-season C_4 dominant, mixed C_3 and C_4 species, and cool-season

C_3 dominant), and climate (semi-arid, temperate/temperate continental, humid continental, and Mediterranean). Long term MAT ranged from 5 to 17 °C and MAP ranged from 345 to 1455 mm across sites. General site characteristics for the study sites are provided in Table 1. Detailed site information can be found in previous studies (see references in Table 1) or AmeriFlux website (http://ameriflux.ornl.gov/).

2.2. Meteorological, eddy flux, and MODIS EVI data

Site-specific climate data [i.e., air temperature (T_a), precipitation, volumetric soil water content (SWC), vapor pressure deficit (VPD)] and Level-4 eddy flux (half hourly, daily, and weekly) were acquired from the AmeriFlux website (http://ameriflux.ornl.gov/) or from published data by the site PI (R. Scott, Kendall grassland). Carbon and water vapor fluxes were measured at each site using the eddy covariance technique. GPP was derived by partitioning NEE data (Reichstein et al., 2005). Some study sites (Flagstaff Wildfire, El Reno burn and control, Fermi Prairie, Walnut, and Brookings) had a total of only two to three years of data and measurements were not available for the entire year (mainly missing during winter, non-growing season). In this case, NEE, GPP, ER, and ET data over the available period were averaged for the same date into a single composite year and integrated for the entire year to derive annual sums of NEE (NEE_{yr}), GPP (GPP_{yr}), ER (ER_{yr}), and ET (ET_{yr}) at each site. Moreover, due to data availability during most of the growing season, growing season sums of NEE (NEE_{GSL}), GPP (GPP_{GSL}), ER (ER_{GSL}), and ET (ET_{GSL}) at each site were also computed for each year. For the rest of the sites where multiple years of data were available for the entire year, annual and growing season sums of carbon fluxes and ET at each site were computed for each year. Since flux data were available for the peak growing season across all site-years, maximum values of fluxes (NEE_{max}, GPP_{max}, and ET_{max}) at each site were computed for each year.

The 8-day composite MODIS land surface reflectance (MOD09A1) data for single pixels (500 m x 500 m) containing the geo-location coordinates of a flux tower were downloaded from the data portal of the Earth Observation and Modeling Facility, the University of Oklahoma (http://eomf.ou.edu/visualization/). Although the spatial resolution of the MODIS pixels and flux tower footprints may vary, Figure S2 shows that the MODIS pixels mostly cover uniform grasslands. Blue, green, red, and near infrared (nir) bands were used to derive EVI (Huete et al., 2002) as shown below:

$$EVI = 2.5 \times \frac{\rho_{nir} - \rho_{red}}{\rho_{nir} + (6 \times \rho_{red} - 7.5 \times \rho_{blue}) + 1} \quad (1)$$

where ρ is surface reflectance in the wavelength band. EVI, widely used as a proxy of canopy greenness, is an optimized version of normalized difference vegetation index (NDVI) to account for atmospheric noise variations and variable soil and canopy background influences (Huete et al., 2002).

To match the temporal resolution of EVI, we calculated 8-day composite values of fluxes and meteorological variables. We averaged 8-day composite values of NEE, GPP, ET, T_a, and SWC over the study period for the same date into a single composite year for each site to determine their mean seasonal patterns. Maximum values of EVI (EVI_{max}) during the growing season were computed for each year. The 8-day composite EVI values for the growing season were summed to derive growing season sum of EVI (EVI_{sum}) for each year.

2.3. Growing season length based on GPP and EVI

Growing season length based on GPP (GSL_{GPP}) was determined as the number of days for which GPP was > 1 g C m^{-2} day^{-1} (Wagle et al., 2014). Carbon uptake period (CUP) was determined as the number of days of negative NEE (carbon uptake by the ecosystem) during the

160 growing season (Wagle et al., 2015). If there were periods with GPP less than 1 g C m^{-2} day^{-1} or
161 positive NEE during the growing season, those periods were excluded from GSL_{GPP} or CUP (for
162 example see Brookings site in Table 2). To relate GSL_{GPP} from flux tower measurements, the
163 growing season length (GSL_{EVI}) was determined based on EVI. The GSL_{EVI} was defined as the
164 number of days the EVI was greater than the given threshold values for each site. The threshold
165 values of EVI were determined when EVI started to increase at the beginning of the growing
166 season and decreased after senescence. The threshold EVI values were ~0.12 at semi-arid sites
167 (Audubon, Flagstaff, and Kendall) and Fortpeck, while they were ~ 0.20 at all other sites. To
168 reduce the uncertainties in times series of EVI and interannual variations in the growing season
169 length at individual sites (the green-up time of grassland links to timing of rainfall and spring
170 temperature), we averaged 8-day composite EVI and carbon fluxes over the study period into a
171 single composite year to produce mean 8-day time series of EVI and carbon fluxes, then
172 determined GSL_{EVI}, GSL_{GPP}, and CUP.

173 *2.4. Calculation of ecosystem water use efficiency (EWUE)*

174 The EWUE for the annual scale ($EWUE_{yr}$) was calculated from the ratio of GPP_{yr} to ET_{yr},
175 while EWUE for the growing season ($EWUE_{GSL}$) was determined from the ratio of integrated
176 GPP (GPP_{GSL}) to ET (ET_{GSL}) over the growing season. To assess the intrinsic link between GPP
177 and ET via stomatal conductance at the ecosystem level, inherent ecosystem water use efficiency
178 (IEWUE) was derived from the ratio of GPP to ET multiplied by VPD on daily time scales (Beer
179 et al., 2009) and compared for selected sites in different climate zones during dry years. To
180 further examine the relative response of NEE, GPP, and ET to two major climatic variables (T_a
181 and VPD) across study sites, half-hourly daytime (global radiation > 5 W m^{-2}) NEE, GPP, and

ET during the period of GSL_{GPP} (Table 2) for the entire study period were aggregated in 10 classes of increasing T_a and VPD, and plotted against T_a and VPD.

2.5. Statistical analysis

We performed correlation and regression analyses between fluxes, EVI, and major climatic variables to assess the degree of association between dependent and independent variables. The relationships with the highest level of significance (i.e., best fit functions) were selected. The coefficient of variation (*CV*) was calculated for annual and seasonal integrals and maximum values of fluxes and EVI across study sites to characterize the magnitudes of spatial variations.

3. Results

3.1. Climatic conditions across study sites

Air temperature showed similar seasonal patterns across study sites, while volumetric SWC showed different seasonal patterns among study sites (Fig. 1). Annual average SWC was below 20% at semi-arid sites, 25-35% at temperate and temperate-continental sites, 44% at Brookings (humid continental), and 18% at Vaira (Mediterranean). Annual average relative water content [$\theta_R = (\theta - \theta_{min})/(\theta_{max} - \theta_{min})$, where θ_{min} and θ_{max} are minimum and maximum values of soil water content observed at each site] was low at semi-arid sites (0.34 at Audubon, 0.39 at Flagstaff, and 0.34 at Kendall), while it was 0.43 at Vaira and > 0.46 at other sites (up to 0.65 at Brookings) (data not shown).

Several study sites experienced drought during the study period. For example, annual rainfall in 2004 was 26% lower than in 2005 at Audubon. At El Reno, annual rainfall was ~ 30 % below the annual average (860 mm, 1971-2000) in both years of the study period. However, growing season rainfall and SWC at El Reno were higher in 2005 than 2006 (Fischer et al., 2012). Annual rainfall in 2012 was 60% lower than in 2010 at Konza. Annual rainfall in 2001 was 33% lower

than in 2003 at Fort Peck. The Goodwin site received more than normal rainfall in 2004 but experienced drought in 2005. At Vaira, annual rainfall in the hydrological year (July to June) of 2003-2004 was 44% lower than the hydrological year of 2004-2005.

3.2. Seasonality and magnitudes of EVI and carbon and water vapor fluxes, and climatic controls

To characterize the seasonal variation of grassland phenology, the mean seasonal cycles of EVI, GPP, and ET were determined (Fig. 2). The EVI generally began to increase rapidly at approximately DOY 100 (April) for the majority of the sites, reached peak values in summer (peak growth), and decreased during the plant senescence stage and approached the pre-CUP value (e.g., prior to DOY 100) near DOY 300 (end of October). However, different seasonal lengths, as indicated by seasonal dynamics of EVI, were observed at Audubon and Kendall (semi-arid grasslands: DOY 180-300, corresponding to the summer rainy season), Vaira (Mediterranean grassland: ~DOY 300-160, with EVI_{max} occurring in spring), and Goodwin (temperate: ~DOY 25-335). Table 2 shows that mean EVI_{max} ranged from 0.27 ± 0.08 (Kendall) to 0.66 ± 0.1 (Brookings) and mean seasonal EVI_{sum} ranged from 2.49 ± 0.27 (Kendall) to 16.28 ± 0.22 (Goodwin), with *CV* of 31 and 48% across sites, respectively. The across-site analysis shows that EVI_{max} was strongly correlated with annual average $\square_R$ ($R^2 = 0.70$, $P < 0.001$) but not with seasonal average $\square_R$ ($R^2 = 0.12$, $P = 0.27$). Similarly, mean seasonal EVI_{sum} was strongly correlated with spatial variation in annual average $\square_R$ ($R^2 = 0.67$, $P = 0.001$) than seasonal average $\square_R$ ($R^2 = 0.17$, $P = 0.18$). Annual average $\square_R$ and MAP together explained 90% ($P < 0.0001$) of spatial variation in mean seasonal EVI_{sum}.

The seasonal dynamics of carbon and water vapor fluxes also corresponded well with the vegetation dynamics because the fluxes began to increase after the grasses greened up, peaked at

the maturity stage, and declined after senescence (Fig. 2). The GSL_{GPP} varied from only about 1.5 months (from end of July to mid-September) at semi-arid sites (Audubon and Kendall grasslands) to about nine months (from the starting of February to early November) at Goodwin (Table 2). Similarly, CUP was the longest (eight months) at Goodwin and the shortest at Audubon (41 days) as CUP was strongly correlated with GSL_{GPP} ($R^2 = 0.65$, $P < 0.001$) and MAP ($R^2 = 0.72$, $P < 0.001$). As expected, strong correlations were observed between GPP_{yr} or GPP_{GSL} and GSL_{GPP} (both: $R^2 = 0.79$, $P < 0.001$), and between CUP and NEE_{yr} ($R^2 = 0.66$, $P = 0.001$) or NEE_{GSL} ($R^2 = 0.56$, $P = 0.005$). Different magnitudes of NEE, GPP, and ET were observed across study sites (Table 2), with *CV* of 51%, 42%, and 29%, respectively, indicating a larger spatial variability of NEE and GPP than of ET. Annual average $\square_R$ explained 22% ($P = 0.11$), 33% ($P = 0.05$), and 74% ($P < 0.0001$) of spatial patterns in NEE_{max}, GPP_{max}, and ET_{max}, respectively.

3.3. Variability in carbon and water budgets

Large variability in annual and seasonal sums of NEE, GPP, and ET was observed across study sites (Table 3), with CV of 164%, 54%, and 39%, respectively, on an annual scale and 93%, 58%, and 46%, respectively, on the seasonal scale. Average NEE_{yr} across study sites showed a net carbon uptake by grasslands, -76 ± 125 (± SD) g C m^{-2} $year^{-1}$, but with larger variability than the uptake itself. The spatial variation in NEE_{yr} was more strongly related to the variation in GPP_{yr} ($R^2 = 0.55$, $P = 0.006$) than to ecosystem respiration (ER_{yr}, $R^2 = 0.33$, $P = 0.05$). Annual and seasonal sums of carbon fluxes and ET tended to be lower in regions with smaller precipitation as fluxes showed positive and nonlinear relationship with precipitation (Fig. 3). Results show that GPP, ER, and ET were similar for the site-years with approximately > 800 mm of annual precipitation and > 600 mm of seasonal precipitation. The across-site analysis

shows that annual average $\square_R$ explained 53% ($P = 0.01$) of NEE_{GSL}, 55% ($P < 0.01$) of NEE_{yr}, 72% ($P < 0.001$) of GPP_{GSL} and ER_{GSL}, 75% ($P < 0.001$) of GPP_{yr}, and 67% ($P = 0.002$) of ER_{yr} when the Brookings site was excluded. Annual average $\square_R$ explained 77% ($P < 0.001$) and 74% ($P < 0.001$) of spatial variations in ET_{GSL} and ET_{yr}, respectively.

In addition to spatial variability, grasslands showed large interannual variability in carbon uptake potential in response to climate forcing (i.e., drought) and disturbances (i.e., fire, invasion) or the biological legacy effects of extensive vegetation growth in the previous year. For example, there was a net carbon uptake of 167 g C m^{-2} $year^{-1}$ at the Audubon site in 2005 when annual and seasonal rainfall was over 350 and 250 mm, respectively, while the site emitted more carbon than it assimilated for the rest of the years. The Konza site, which had a consistent carbon uptake from 2007 to 2011, emitted more carbon than it assimilated in the drought year of 2012. The Flagstaff Wildfire site emitted more carbon than it assimilated both on seasonal and annual time scales for the entire study period because of the wildfire a decade before the flux measurements that killed all trees. The Audubon site emitted more carbon in 2003 after the wildfire in 2002. The carbon uptake by the Fermi Prairie site declined dramatically in 2006 because of an infestation of white sweet clover (*Melilotus alba*) which died out completely and very little green vegetation was left in the field after July. Even though spring 2006 was wet at the Vaira site, NEE decreased substantially in the 2005-2006 growing season because an extraordinary amount of litter produced in 2004-2005 covered the ground surface and suppressed the grass growth in 2005-2006, and also increased ER (Ma et al., 2007).

3.4. Relationship of EVI with carbon and water vapor fluxes

The EVI was strongly correlated with GPP, with correlation coefficient (r) of more than 0.8 at nine out of 12 sites, and with ET, with r of more than 0.7 at ten out of 12 sites (Table 4). The

across-site analysis showed that the correlation of EVI remained high with seasonal variations in GPP (r = 0.85) and ET (r = 0.80). The EVI_{max} was strongly correlated with spatial variations in NEE_{max} (R^2 = 0.67, *P* = 0.001), GPP_{max}, (R^2 = 0.80, *P* < 0.001), and ET_{max} (R^2 = 0.68, *P* < 0.001). To further test the capabilities of EVI to capture the observed trends in the flux data series and seasonal sums of fluxes, we tested the ability of GSL_{EVI} to predict GSL_{GPP} and CUP (Fig. 4a), and seasonal sums of GPP and ET (Fig. 4b). We also examined the relationships of EWUE, GPP, and ET with EVI_{sum} on the seasonal scale (Fig. 4c, d). The GSL_{EVI} showed strong linear correlations with the spatial variability in GSL_{GPP} (R^2 = 0.94, *P* < 0.0001), CUP (R^2 = 0.70, *P* < 0.001), GPP_{GSL} (R^2 = 0.62, *P* = 0.002), and ET_{GSL} (R^2 = 0.61, *P* = 0.003). High levels of canopy green biomass and coverage, as indicated by higher seasonal EVI_{sum}, were strongly associated with higher $EWUE_{GSL}$ (R^2 = 0.62, *P* < 0.0001), GPP_{GSL} (R^2 = 0.78, *P* < 0.0001), and ET_{GSL} (R^2 = 0.73, *P* < 0.0001) (Fig. 4c, d).

3.5. Relationship between GPP and ET, and variability in EWUE

The across-site analysis of annual or growing season sums of GPP and ET showed strong positive relationships (R^2 = 0.77 on an annual scale and R^2 = 0.82 on the seasonal scale, Fig. 5), indicating strong coupling between GPP and ET. However, the ratio of sums of GPP to ET yielded variations in $EWUE_{yr}$ (ranged from 0.67 ± 0.55 to 2.52 ± 0.52 g C mm^{-1} ET) and $EWUE_{GSL}$ (ranged from 0.90 ± 0.36 to 2.65 ± 0.43 g C mm^{-1} ET) across study sites (Table 3). We also found interannual variability in EWUE at the same sites. Reduction in GPP during relatively dry years compared to non-dry years at a similar level of ET resulted in a smaller EWUE (i.e., the slope of the relationship between GPP and ET, Fig. 6).

3.6. *Response of NEE, GPP, and ET to T_a and VPD*

296 To better understand the effects of climate change on carbon and water vapor fluxes of
297 grassland ecosystems, we compared the response of NEE, GPP, and ET to two major climatic
298 variables (T_a and VPD) among all grassland sites (Fig. 7a, b). Results show that the responses of
299 NEE, GPP, and ET to T_a and VPD varied among grassland sites. In general, NEE, GPP, and ET
300 increased with T_a and VPD up to a certain level and declined thereafter. The optimum ranges of
301 T_a and VPD for NEE, GPP, and ET differed among sites. However, the responses of NEE, GPP,
302 and ET to T_a and VPD were very similar among grasslands in the same climatic zone. Maximum
303 values of NEE, GPP, and ET occurred at about 22-23 °C at two semi-arid sites (Flagstaff
304 Wildfire and Kendall), while they occurred at ~27 °C at another semi-arid site (Audubon).
305 Maximum values of NEE and GPP occurred at ~25 °C and ET occurred at ~30 °C at Fermi
306 Prairie, while NEE and GPP peaked at ~30 °C and ET peaked at ~35 °C at all other four
307 temperature continental sites and Goodwin (temperate). The NEE and GPP peaked at ~25 °C and
308 ET at ~30 °C at Brookings and Fort Peck. Maximum values of NEE, GPP, and ET occurred at
309 ~20 °C at Vaira (Mediterranean).
310 Maximum values of NEE, GPP, and ET occurred at about VPD of 15-17 hPa and depressed
311 when VPD > 20 hPa at all three semi-arid sites. The values reached maximum at ~27 hPa at
312 three temperate continental sites (El Reno burn, El Reno control, and Konza), while they were
313 maximum at ~20 hPa at Walnut and ~15 hPa at Fermi Prairie. Both NEE and GPP reached
314 maximum at ~10 hPa at Brookings, Fort Peck, and Vaira, while they reached maximum at ~18
315 hPa at Goodwin. The ET reached maximum at ~25 hPa at Brookings, ~20 hPa at two temperate
316 sites (Fort Peck and Goodwin), and at ~15 hPa at Vaira. Our results show that carbon fluxes and
317 ET responded to T_a and VPD differently. Lower optimum temperature ranges for NEE and GPP
318 than ET, and more decline in NEE and GPP than ET at high T_a and VPD across sites (Fig. 7a, b)

319 indicated that physiological controls in response to increased T_a and VPD more greatly affected
320 NEE and GPP than ET.

321 As the individual response of GPP and ET to climatic variables may be confounded by the
322 effect of VPD on canopy conductance, we also compared the relationship between GPP and ET
323 vs. GPP x VPD and ET at the three selected sites in different climatic zones during relatively dry
324 years (Fig. 8). As expected, GPP and ET showed a linear relationship, but interestingly the
325 relationship between GPP x VPD and ET was exponential across all sites. The linear relationship
326 (R^2 = 0.82) between GPP and ET was only slightly weaker than the exponential relationship (R^2
327 = 0.84) between GPP x VPD and ET at the El Reno control site, but the exponential relationship
328 between GPP x VPD and ET was substantially stronger than the linear relationship between GPP
329 and ET at Fort Peck (R^2 = 0.70 vs. 0.55) and Vaira (R^2 = 0.86 vs. 0.78).

330 **4. Discussion**

331 *4.1. Variability in EVI and carbon and water vapor fluxes*

332 The considerable effects of precipitation and SWC on vegetation production, as indicated by
333 EVI values, were consistent with previous reports that higher precipitation promotes higher
334 biomass in grasslands across spatial scales (Bai et al., 2004; Sala et al., 1988). This enhanced
335 plant growth and productivity was strongly correlated with greater rates of carbon and water
336 vapor fluxes, showing the ability of EVI to track spatial variability in carbon and water vapor
337 fluxes of geographically-distributed grasslands. Our analysis also demonstrates that EVI can be
338 used to delineate growing season length and CUP, and to approximate carbon and water vapor
339 fluxes, and EWUE of grasslands (Fig. 4). These results indicate much potential of using this EVI
340 approach for understanding and extrapolating fluxes over large grassland areas. A previous study
341 also showed the potential to link the MODIS EVI and tower-derived GPP to better understand

342 the functioning of savanna ecosystems across the north Australian tropical transect (Ma et al.,
343 2013). Similarly, Churkina et al. (2005) showed that EVI calculated from VEGETATION
344 SPOT-4 was strongly correlated to the CUP and could be utilized to estimate NEE_{yr} of a broad
345 range of ecosystems.

346 Our results illustrate that the carbon uptake-emission status of the grasslands was conditional
347 upon soil water availability and precipitation. Higher annual average $\square_R$ was strongly correlated
348 with higher values of fluxes. Similarly, carbon fluxes and ET increased linearly with increasing
349 precipitation at lower ranges of precipitation (< 1000 mm of annual rainfall and < 600 mm of
350 seasonal rainfall) (Fig. 3). This result supports an earlier finding (Gilmanov et al., 2005) that
351 mixed prairie ecosystems in North America emitted more carbon than they assimilated during
352 years with lower than normal rainfall. A study that manipulated rainfall variability and quantity
353 in a C_4 dominated native grassland in Northeast Kansas showed that carbon cycling processes
354 such as soil carbon efflux and carbon uptake by the vegetation were suppressed when rainfall
355 variability increased (Knapp et al., 2002). These results indicate that projected increases in
356 rainfall variability due to anthropogenic climate change and atmospheric warming could greatly
357 influence carbon cycling processes of grasslands. Further, our study shows that carbon dynamics
358 of grasslands were subject to disturbance events (*i.e.*, fire, invasion) and the biological legacy
359 effects of one year on another year. Such alterations in carbon dynamics have been reported for
360 several grassland and forest ecosystems worldwide (Amiro et al., 2006; Barr et al., 2007; Ciais et
361 al., 2005; Flanagan et al., 2002; Gilmanov et al., 2007). These results suggest that this
362 interannual variability in carbon and water vapor fluxes of ecosystems should be considered
363 when estimating regional carbon and water budgets.

364 *4.2. Coupling between GPP and ET, and variability in EWUE*

As expected, GPP and ET were strongly correlated (Fig. 5) due to the physiological control of gas exchange (Valentini et al., 1991). However, responses to seasonal variations in climatic variables differed between GPP and ET. These differential responses presumably led to partial decoupling between GPP and ET under changing environmental conditions. As a result, the relationship between GPP and ET was weaker as compared to GPP x VPD and ET among selected sites in different climatic zones in relatively dry years (Fig. 8). These results demonstrate that the intrinsic link between carbon assimilation and water loss through stomatal conductance exists in grasslands at the ecosystem level since the ratio of ET to VPD is a proxy for canopy conductance (Beer et al., 2009). As in Beer et al. (2009), we also observed a nonlinear relationship between GPP x VPD and ET for grasslands, suggesting greater decoupling of herbaceous canopies from the atmosphere than forests (Jarvis and McNaughton, 1986).

The climatic gradient affected grassland phenology and canopy coverage across study sites, which strongly influenced carbon and water vapor fluxes of grasslands. The GPP_{GSL} and ET_{GSL} were strongly correlated with EVI_{sum}, and additional units of EVI were associated with a greater increase in GPP_{GSL} (101 g C m^{-2}) than ET_{GSL} (43.3 mm) as shown in Figure 4d. This is likely because increasing canopy coverage increased light use efficiency for photosynthesis and attenuated radiation transmitted to the soil surface and reduced soil evaporation. Although both GPP and ET decreased during dry conditions, drought-induced reduction in vegetation cover along with leaf-level physiological controls of high T_a and VPD on GPP than on ET caused more reduction in GPP than in ET. As a result, EWUE was higher at the sites with larger EVI and less climatically-imposed water limitation, and it was lower in dry years (Fig. 6) and at sites with smaller EVI (Fig. 4c). Our result supports the finding of a previous study (Hu et al., 2008) which showed a reduction in EWUE during drought and high EWUE in the years or sites with high

388 productivity of Chinese temperate grasslands. These results show a pronounced effect of drought
389 on carbon and water vapor fluxes and EWUE of grasslands.

390 Reduction in EWUE of grasslands during drought in this study indicated the opposite
391 response than what has generally been reported for forests. Previous studies in forest ecosystems
392 have shown that EWUE of forests increases in dry years because of a greater reduction in ET
393 than GPP. During drought, EWUE increased in European forests but not in grasslands (Wolf et
394 al., 2013). Krishnan et al. (2006) reported a larger relative reduction in ET than in GPP of boreal
395 forests in Saskatchewan, Canada, leading to higher EWUE in dry years. Likewise, fairly constant
396 values of EWUE were observed in most of the coniferous boreal and temperate forests of Canada
397 (Brümmer et al., 2012). Water use efficiency in a beech forest was mainly controlled by
398 evaporative demand of the atmosphere and leaf stomatal behavior, and not by the canopy
399 coverage (Herbst et al., 2002). In contrast, higher EWUE of grasslands was associated with
400 higher EVI in our study (Fig. 4c). This contrasting result can be attributed to differences in soil
401 evaporation as soil evaporation is negligible under well-developed forest but considerable in
402 grasslands. Previous studies reported that grasslands did not reduce ET as long as soil moisture
403 was available but forests employed water saving strategies by reducing ET, causing the
404 contrasting responses of European forests and grasslands to drought and heatwaves (Teuling et
405 al., 2010; Wolf et al., 2013). These results suggest that the current ecosystem modeling
406 approaches which predict increasing EWUE in response to drought (Baldocchi, 1997; Schulze,
407 1986; Williams et al., 1998) under the assumption of more stomatal regulation of water losses
408 with slight reductions in photosynthesis (Flexas and Medrano, 2002) might not be applicable for
409 all biomes, at least for grasslands. This indicates the need to consider reduction in EWUE during
410 drought when modeling carbon fluxes of grasslands, especially in drought-prone environments.

5. Conclusions

This study revealed large spatial variability in carbon and water vapor fluxes, and vegetation properties such as EVI among geographically-distributed grasslands in the U.S. These variations were primarily related to differences in precipitation and soil water availability. Integration of EVI with ground-based eddy flux and climate data showed potential to improve understanding of the temporal and spatial variability in carbon and water vapor fluxes, and to approximate GSL, CUP, EWUE, and carbon and water vapor fluxes of grasslands. However, this result needs verification by long-term observations across geographical sites and by more complete sampling of grasslands of the world to examine whether these relationships hold. For example, this study lacks data from grasslands in tropical and sub-tropical regions. Our results show that the optimum T_a and VPD ranges were lower for NEE and GPP than for ET, and NEE and GPP were reduced more than ET at high T_a and VPD, suggesting the higher sensitivity of NEE and GPP than ET to aridity. As a result, EWUE of grasslands decreased during dry years, a response the opposite of what has generally been reported in forest ecosystems. This result is inconsistent with the assumption of current models of canopy functions which predict increasing EWUE during drought due to a reduction in stomatal conductance. An evaluation of the intrinsic link between GPP and ET through stomatal conductance across a wide range of environmental conditions is essential to better understand adaptation mechanisms of grasslands to climate. Our study's comparison of the responses of carbon and water vapor fluxes of geographically-distributed grasslands to major climatic variables provides insight about the effects of climate change on carbon and water budgets of grasslands.

Acknowledgement

This study was supported in part by a research grant (Project No. 2012-02355) through the USDA National Institute for Food and Agriculture (NIFA)'s Agriculture and Food Research Initiative (AFRI), Regional Approaches for Adaptation to and Mitigation of Climate Variability and Change, and a research grant (IIA-1301789) from the National Science Foundation EPSCoR. This research was supported by grants to T. Kolb and Northern Arizona University from the North American Carbon Program/USDA CREES NRI (2004-35111-15057 and 2008-35101-19076) and Science Foundation Arizona (CAA 0-203-08). The Konza Prairie site was supported by grants to N. Brunsell from the NSF EPSCoR (NSF EPS- 0553722 and EPS-0919443) and KAN0061396/KAN0066263 and the NSF Long Term Ecological Research Program at Konza Prairie Biological Station (DEB-0823341 and sub-contract: SS1093). It was also partly supported by NOAA Climate Program Office's Sectoral Applications Research Program (SARP) grant NA130AR4310122. The Fermi site was supported by the U.S. Department of Energy, Office of Science, Office of Biological and Environmental Research, Terrestrial Ecosystem Science Program under contract DE-AC02-06CH11357. Funding for the Kendall and Santa Rite flux sites was from the USDA and U.S. Department of Energy's Office of Science. Data were obtained from AmeriFlux database (http://ameriflux.ornl.gov/). The authors thank an anonymous reviewer for the comments on previous version of this manuscript.

References

Amiro, B. et al., 2006. Carbon, energy and water fluxes at mature and disturbed forest sites, Saskatchewan, Canada. Agricultural and Forest Meteorology, 136(3): 237-251.

Bai, Y., Han, X., Wu, J., Chen, Z. and Li, L., 2004. Ecosystem stability and compensatory effects in the Inner Mongolia grassland. Nature, 431(7005): 181-184.

Baldocchi, D., 1997. Measuring and modelling carbon dioxide and water vapour exchange over a temperate broad-leaved forest during the 1995 summer drought. Plant, Cell & Environment, 20(9): 1108-1122.

Baldocchi, D.D., Xu, L. and Kiang, N., 2004. How plant functional-type, weather, seasonal drought, and soil physical properties alter water and energy fluxes of an oak–grass savanna and an annual grassland. Agricultural and Forest Meteorology, 123(1): 13-39.

Barr, A.G. et al., 2007. Climatic controls on the carbon and water balances of a boreal aspen forest, 1994–2003. Global Change Biology, 13(3): 561-576.

Beer, C. et al., 2009. Temporal and among-site variability of inherent water use efficiency at the ecosystem level. Global Biogeochemical Cycles, 23(2).

Biondini, M.E., Lauenroth, W.K. and Sala, O.E., 1991. Correcting estimates of net primary production: are we overestimating plant production in rangelands. Journal of Range Management, 44(3): 194-198.

Brümmer, C. et al., 2012. How climate and vegetation type influence evapotranspiration and water use efficiency in Canadian forest, peatland and grassland ecosystems. Agricultural and Forest Meteorology, 153: 14-30.

Brunsell, N.A., Ham, J.M. and Owensby, C.E., 2008. Assessing the multi-resolution information content of remotely sensed variables and elevation for evapotranspiration in a tall-grass prairie environment. Remote Sensing of Environment, 112(6): 2977-2987.

Burkett, V.R. et al., 2005. Nonlinear dynamics in ecosystem response to climatic change: case studies and policy implications. Ecological complexity, 2(4): 357-394.

Churkina, G., Schimel, D., Braswell, B.H. and Xiao, X., 2005. Spatial analysis of growing season length control over net ecosystem exchange. Global Change Biology, 11(10): 1777-1787.

Ciais, P. et al., 2005. Europe-wide reduction in primary productivity caused by the heat and drought in 2003. Nature, 437(7058): 529-533.

DeForest, J.L. et al., 2006. Phenophases alter the soil respiration–temperature relationship in an oak-dominated forest. International journal of biometeorology, 51(2): 135-144.

Dore, S. et al., 2008. Long-term impact of a stand-replacing fire on ecosystem CO2 exchange of a ponderosa pine forest. Global Change Biology, 14(8): 1801-1820.

Falge, E. et al., 2002. Phase and amplitude of ecosystem carbon release and uptake potentials as derived from FLUXNET measurements. Agricultural and Forest Meteorology, 113(1): 75-95.

Fischer, M.L. et al., 2012. Carbon, water, and heat flux responses to experimental burning and drought in a tallgrass prairie. Agricultural and Forest Meteorology, 166: 169-174.

Flanagan, L.B., Wever, L.A. and Carlson, P.J., 2002. Seasonal and interannual variation in carbon dioxide exchange and carbon balance in a northern temperate grassland. Global Change Biology, 8(7): 599-615.

493 Flexas, J. and Medrano, H., 2002. Drought-inhibition of photosynthesis in C3 plants: stomatal
494 and non-stomatal limitations revisited. Annals of Botany, 89(2): 183-189.
495 Gill, R.A. et al., 2002. Nonlinear grassland responses to past and future atmospheric CO2.
496 Nature, 417(6886): 279-282.
497 Gilmanov, T. et al., 2007. Partitioning European grassland net ecosystem CO2 exchange into
498 gross primary productivity and ecosystem respiration using light response function analysis.
499 Agriculture, Ecosystems & Environment, 121(1): 93-120.
500 Gilmanov, T.G. et al., 2010. Productivity, respiration, and light-response parameters of world
501 grassland and agroecosystems derived from flux-tower measurements. Rangeland Ecology
502 & Management, 63(1): 16-39.
503 Gilmanov, T.G. et al., 2005. Integration of CO2 flux and remotely-sensed data for primary
504 production and ecosystem respiration analyses in the Northern Great Plains: Potential for
505 quantitative spatial extrapolation. Global Ecology and Biogeography, 14(3): 271-292.
506 Gilmanov, T.G. et al., 2003. Gross primary production and light response parameters of four
507 Southern Plains ecosystems estimated using long-term CO2-flux tower measurements.
508 Global Biogeochemical Cycles, 17(2).
509 Herbst, M., Kutsch, W.L., Hummelshøj, P., Jensen, N.O. and Kappen, L., 2002. Canopy
510 physiology: interpreting the variations in eddy fluxes of water vapour and carbon dioxide
511 observed over a beech forest. Basic and Applied Ecology, 3(2): 157-169.
512 Hu, Z. et al., 2008. Effects of vegetation control on ecosystem water use efficiency within and
513 among four grassland ecosystems in China. Global Change Biology, 14(7): 1609-1619.
514 Huete, A. et al., 2002. Overview of the radiometric and biophysical performance of the MODIS
515 vegetation indices. Remote Sensing of Environment, 83(1): 195-213.

Hutyra, L.R. et al., 2007. Seasonal controls on the exchange of carbon and water in an Amazonian rain forest. Journal of Geophysical Research: Biogeosciences (2005–2012), 112(G3).

Huxman, T.E. et al., 2004. Convergence across biomes to a common rain-use efficiency. Nature, 429(6992): 651-654.

Jarvis, P.G. and McNaughton, K., 1986. Stomatal control of transpiration: scaling up from leaf to region. Advances in ecological research, 15: 1-49.

Kato, T. and Tang, Y., 2008. Spatial variability and major controlling factors of CO2 sink strength in Asian terrestrial ecosystems: evidence from eddy covariance data. Global Change Biology, 14(10): 2333-2348.

Knapp, A.K. et al., 2002. Rainfall variability, carbon cycling, and plant species diversity in a mesic grassland. Science, 298(5601): 2202-2205.

Krishnan, P. et al., 2006. Impact of changing soil moisture distribution on net ecosystem productivity of a boreal aspen forest during and following drought. Agricultural and Forest Meteorology, 139(3): 208-223.

Krishnan, P., Meyers, T.P., Scott, R.L., Kennedy, L. and Heuer, M., 2012. Energy exchange and evapotranspiration over two temperate semi-arid grasslands in North America. Agricultural and Forest Meteorology, 153: 31-44.

Law, B. et al., 2002. Environmental controls over carbon dioxide and water vapor exchange of terrestrial vegetation. Agricultural and Forest Meteorology, 113(1): 97-120.

Ma, S., Baldocchi, D.D., Xu, L. and Hehn, T., 2007. Inter-annual variability in carbon dioxide exchange of an oak/grass savanna and open grassland in California. Agricultural and Forest Meteorology, 147(3): 157-171.

539 Ma, X. et al., 2013. Spatial patterns and temporal dynamics in savanna vegetation phenology
540 across the North Australian Tropical Transect. Remote Sensing of Environment, 139: 97-
541 115.
542 Matamala, R., Jastrow, J.D., Miller, R.M. and Garten, C., 2008. Temporal changes in C and N
543 stocks of restored prairie: implications for C sequestration strategies. Ecological
544 Applications, 18(6): 1470-1488.
545 Myneni, R.B., Keeling, C., Tucker, C., Asrar, G. and Nemani, R., 1997. Increased plant growth
546 in the northern high latitudes from 1981 to 1991. Nature, 386(6626): 698-702.
547 Rahman, A.F., Gamon, J.A., Fuentes, D.A., Roberts, D.A. and Prentiss, D., 2001. Modeling
548 spatially distributed ecosystem flux of boreal forest using hyperspectral indices from
549 AVIRIS imagery. Journal of Geophysical Research: Atmospheres (1984–2012), 106(D24):
550 33579-33591.
551 Reichstein, M. et al., 2005. On the separation of net ecosystem exchange into assimilation and
552 ecosystem respiration: review and improved algorithm. Global Change Biology, 11(9):
553 1424-1439.
554 Richardson, A.D. et al., 2010. Influence of spring and autumn phenological transitions on forest
555 ecosystem productivity. Philosophical Transactions of the Royal Society B: Biological
556 Sciences, 365(1555): 3227-3246.
557 Running, S.W. and Hunt, E.R., 1993. Generalization of a forest ecosystem process model for
558 other biomes, BIOME-BGC, and an application for global-scale models. Scaling
559 physiological processes: Leaf to globe: 141-158.
560 Sala, O.E., Parton, W.J., Joyce, L. and Lauenroth, W., 1988. Primary production of the central
561 grassland region of the United States. Ecology, 69(1): 40-45.

562 Schulze, E., 1986. Carbon dioxide and water vapor exchange in response to drought in the
563 atmosphere and in the soil. Annual Review of Plant Physiology, 37(1): 247-274.
564 Scott, R.L., Hamerlynck, E.P., Jenerette, G.D., Moran, M.S. and Barron-Gafford, G.A., 2010.
565 Carbon dioxide exchange in a semidesert grassland through drought-induced vegetation
566 change. Journal of Geophysical Research: Biogeosciences (2005–2012), 115(G3).
567 Song, J., Liao, K., Coulter, R.L. and Lesht, B.M., 2005. Climatology of the low-level jet at the
568 Southern Great Plains Atmospheric Boundary Layer Experiments site. Journal of Applied
569 Meteorology, 44(10).
570 Soussana, J. et al., 2007. Full accounting of the greenhouse gas (CO2, N2O, CH4) budget of nine
571 European grassland sites. Agriculture, Ecosystems & Environment, 121(1): 121-134.
572 Suyker, A.E., Verma, S.B. and Burba, G.G., 2003. Interannual variability in net CO2 exchange
573 of a native tallgrass prairie. Global Change Biology, 9(2): 255-265.
574 Teuling, A.J. et al., 2010. Contrasting response of European forest and grassland energy
575 exchange to heatwaves. Nature Geoscience, 3(10): 722-727.
576 Turner, D.P. et al., 2003. Scaling Gross Primary Production (GPP) over boreal and deciduous
577 forest landscapes in support of MODIS GPP product validation. Remote Sensing of
578 Environment, 88(3): 256-270.
579 Valentini, R., Scarascia Mugnozza, G., ANGELLS, P. and Bimbi, R., 1991. An experimental test
580 of the eddy correlation technique over a Mediterranean macchia canopy. Plant, Cell &
581 Environment, 14(9): 987-994.
582 Wagle, P., Xiao, X. and Suyker, A.E., 2015. Estimation and analysis of gross primary production
583 of soybean under various management practices and drought conditions. ISPRS Journal of
584 Photogrammetry and Remote Sensing, 99(0): 70-83.

585 Wagle, P. et al., 2014. Sensitivity of vegetation indices and gross primary production of tallgrass
586 prairie to severe drought. Remote Sensing of Environment, 152(0): 1-14.
587 Williams, M. et al., 1998. Seasonal variation in net carbon exchange and evapotranspiration in a
588 Brazilian rain forest: a modelling analysis. Plant, Cell & Environment, 21(10): 953-968.
589 Wolf, S. et al., 2013. Contrasting response of grassland versus forest carbon and water fluxes to
590 spring drought in Switzerland. Environmental Research Letters, 8(3): 035007.
591 Xiao, J. et al., 2014. Data-driven diagnostics of terrestrial carbon dynamics over North America.
592 Agricultural and Forest Meteorology, 197: 142-157.
593 Xiao, J. et al., 2008. Estimation of net ecosystem carbon exchange for the conterminous United
594 States by combining MODIS and AmeriFlux data. Agricultural and Forest Meteorology,
595 148(11): 1827-1847.
596 Yu, G.R. et al., 2013. Spatial patterns and climate drivers of carbon fluxes in terrestrial
597 ecosystems of China. Global change biology, 19(3): 798-810.
598 Yuan, W. et al., 2009. Latitudinal patterns of magnitude and interannual variability in net
599 ecosystem exchange regulated by biological and environmental variables. Global Change
600 Biology, 15(12): 2905-2920.
601 Zhang, X. et al., 2003. Monitoring vegetation phenology using MODIS. Remote sensing of
602 environment, 84(3): 471-475.
603
604

Figure Legends:

Fig. 1. Mean seasonal dynamics (8-day composite values) of annual air temperature and near surface volumetric soil water content (SWC) at the 12 grassland sites. Data over the study period were composited into a single year for each site to determine the mean seasonal patterns.

Fig. 2. Mean seasonal dynamics (8-day composite values) of enhanced vegetation index (EVI), gross primary production (GPP), and evapotranspiration (ET) at the 12 grassland sites. Data over the study period were composited into a single year for each site to determine the mean seasonal patterns.

Fig. 3. Relationships of annual (yr) or growing season (GSL) sums of gross primary production (GPP), ecosystem respiration (ER), and evapotranspiration (ET) with annual or seasonal sum of precipitation (Precip): (a) $y = -313 + 2.23x – 0.0007x^2$, $R^2 = 0.79$, (b) $y = -456 + 3.6x – 0.002x^2$, $R^2 = 0.77$, (c) $y = -215 + 1.95x – 0.0006x^2$, $R^2 = 0.74$, (d) $y = -274 + 2.59x – 0.001x^2$, $R^2 = 0.79$, (e) $y = 31.76 + 1.01x – 0.0004x^2$, $R^2 = 0.50$, and (f) $y = -103 + 1.67x – 0.001x^2$, $R^2 = 0.62$. All relationships were statistically significant at the 0.0001 level. Lines represent best fit regressions.

Fig. 4. Relationships between: (a) carbon uptake period (CUP) and growing season lengths based on enhanced vegetation index (GSL_{EVI}) and gross primary production (GSL_{GPP}): $CUP = 0.9x – 76.2$, $R^2 = 0.70$, $P < 0.001$ and $GSL_{GPP} = 1.18x – 76.02$, $R^2 = 0.94$, $P < 0.0001$, (b) GSL_{EVI} and growing season sums of GPP (GPP_{GSL}) and ET (ET_{GSL}): $GPP_{GSL} = 6.48x – 546$, $R^2 = 0.62$, $P = 0.002$ and $ET_{GSL} = 2.94x – 157$, $R^2 = 0.61$, $P = 0.003$, (c) ecosystem water use efficiency ($EWUE_{GSL}$) and sum of enhanced vegetation index (EVI_{sum}) on the seasonal scale : $y = -0.07 + 0.36x -0.01x^2$, $R^2 = 0.61$, $P < 0.0001$, and (d) GPP_{GSL}, ET_{GSL}, and EVI_{sum}: $GPP_{GSL} = 101x – 109$, $R^2 = 0.78$, $P < 0.0001$ and $ET_{GSL} = 43.3x + 52.7$, $R^2 = 0.73$, $P < 0.0001$. Lines represent best fit regressions.

628 **Fig. 5.** Relationships between annual (yr) or growing season (GSL) gross primary production
629 (GPP) and evapotranspiration (ET) across the 12 grassland sites. Lines represent best fit linear
630 regressions.
631 **Fig. 6.** Ecosystem water use efficiency (EWUE), i.e., the slope of gross primary production
632 (GPP) vs. evapotranspiration (ET) on daily basis in dry (open symbols and dotted lines) and non-
633 dry years (closed symbols and solid lines) for the three selected grassland sites.
634 **Fig. 7.** Response of net ecosystem exchange (NEE), gross primary production (GPP), and
635 evapotranspiration (ET) to (a) air temperature (T_a) and (b) vapor pressure deficit (VPD) at the 12
636 grassland sites. Half-hourly NEE, GPP, and ET data during day time (global radiation > 5 W m^{-2})
637 for the entire study period were aggregated in classes of increasing T_a and VPD.
638 **Fig. 8.** Relationship between gross primary production (GPP) and evapotranspiration (ET), and
639 between GPP x VPD (vapor pressure deficit) and ET on a daily basis for the selected sites during
640 dry years.

641 Table 1. Description of vegetation types and climate at flux sites. MAT: mean annual

642 temperature, MAP: mean annual precipitation.

Climate	Site (State)	Latitude longitude	Elevation (m) MAT (°C) MAP (mm)	Study period	Vegetation	Soil type	References
Semi-arid	Audubon (AZ)	31.5907 -110.5092	1469 14.7 475	2002-2006	Short-grass prairie (C_4) and perennial herbs	Sandy clay loam	Krishnan et al. (2012)
Semi-arid	Flagstaff Wildfire (AZ)	35.4454 -111.7718	2270 9 610	2005-2007	Short-grasses (C_3/C_4 mixed) with a few shrubs	Silt clay loam	Dore et al. (2008)
Semi-arid	Kendall (AZ)	31.7365 -109.9419	1531 17 345	2005-2009	Short-grass prairie (C_4) and C_3 shrubs	Sandy loam	Scott et al. (2010)
Temperate continental	El Reno Burn (OK)	35.5497 -98.0402	421 14.9 860	2005-2006	C_4 dominated tallgrass prairie	Norge silt loam	Fischer et al. (2012)
Temperate continental	El Reno Control (OK)	35.5465 -98.0401	421 14.9 860	2005-2006	C_4 dominated tallgrass prairie	Norge silt loam	Fischer et al. (2012)
Temperate continental	Fermi Prairie (IL)	41.8406 -88.2410	226 9.4 937	2005-2007	C_4 dominated tallgrass prairie	Silt clay loam	Matamala et al. (2008)
Temperate continental	Konza (KS)	39.0824 -96.5603	443 13 835	2007-2012	C_4 dominated tallgrass prairie	Silt clay loam	Brunsell et al. (2008)
Temperate continental	Walnut (KS)	37.5208 -96.8550	408 13.1 1054	2001-2004	Tallgrass prairie (C_3/C_4 mixed)	Silt clay loam	Song et al. (2005)
Humid continental	Brookings (SD)	44.3453 -96.8362	510 5.8 550	2004-2006	Mixed C_3 and C_4 species	Clay loam	Gilmanov et al. (2010)
Temperate	Fort Peck (MT)	48.3077 -105.1019	634 5.13 500	2000-2006 (missing 2002)	Mixed C_3 and C_4 species	Sandy loam	Gilmanov et al. (2010)
Temperate	Goodwin (MS)	34.2547 -89.8735	70 15.7 1455	2002-2006	Short-grasses (C_3/C_4) with scattered trees and shrubs	Silt loam	Gilmanov et al. (2010)
Mediterranean	Vaira (CA)	38.4067 -120.9507	129 15.9 498	2001-2007	Cool-season C_3 species and sparsely distributed oak trees	Very rocky silt loam	Baldocchi et al. (2004)

643

644 Table 2. Seasonal dynamics of carbon fluxes (net ecosystem CO_2 exchange, NEE and gross
645 primary production, GPP), maximum rates of NEE (NEE_{max}, g C m^{-2} day^{-1}), GPP (GPP_{max}, g C
646 m^{-2} day^{-1}), and evapotranspiration (ET_{max}, mm day^{-1}), and maximum (EVI_{max}) and seasonally
647 integrated values (EVI_{sum}) of enhanced vegetation index at the 12 grassland sites.

Site	GSL_{EVI} (DOY)	CUP (DOY)	GSL_{GPP} (DOY)	NEE_{max} (± SD)	GPP_{max} (± SD)	ET_{max} (± SD)	EVI_{max} (± SD)	EVI_{sum} (± SD)
Audubon	185-305	217-257	209-257	-3.59 ± 1.65	5.51 ± 2.57	4.04 ± 1.16	0.32 ± 0.04	3.16 ± 0.24
Flagstaff Wildfire	105-313	121-153	121-273	-0.91 ± 0.34	4.45 ± 0.39	3.39 ± 0.66	0.30 ± 0.04	4.72 ± 0.22
Kendall	193-297	209-257	209-257	-2.73 ± 1.18	4.45 ± 1.45	3.30 ± 0.46	0.27 ± 0.08	2.49 ± 0.27
El Reno burn	97-305	113-217	105-289	-6.85 ± 2.3	13.74 ± 4.82	5.54 ± 0.09	0.54 ± 0.08	10.26 ± 1.33
El Reno control	97-297	113-217	97-289	-5.19 ± 0.23	11.02 ± 2.01	5.69 ± 0.3	0.55 ± 0.09	9.9 ± 1.28
Fermi Prairie	97-313	113-265	105-289	-9.50 ± 1.49	14.49 ± 1.85	5.64 ± 0.34	0.65 ± 0.06	11.68 ± 0.48
Konza	97-321	129-233	97-321	-9.10 ± 1.29	15.86 ± 2.63	7.61 ± 0.92	0.59 ± 0.07	10.31 ± 0.38
Walnut	89-313	113-273	105-289	-4.50 ± 0.77	10.63 ± 0.63	5.24 ± 0.8	0.53 ± 0.05	10.0 ± 0.27
Brookings	81-329	97-185 & 265-305	97-305	-5.35 ± 1.34	10.59 ± 1.62	8.13 ± 1.7	0.66 ± 0.1	13.21 ± 0.05
Fort Peck	97-265	105-169	105-225	-2.12 ± 1.24	4.38 ± 2.14	5.24 ± 2.86	0.31 ± 0.03	4.59 ± 0.17
Goodwin	25-337	33-273	33-313	-6.17 ± 2.29	12.68 ± 1.12	6.41 ± 2.43	0.62 ± 0.04	16.28 ± 0.22
Vaira	305-161	17-137	345-145	-5.41 ± 0.79	10.38 ± 0.60	3.81 ± 0.40	0.43 ± 0.04	8.04 ± 0.51

1. Maximum values of NEE, GPP, ET, and EVI at each site were first determined for an individual year, then averaged for the entire study period.
2. GSL_{EVI} and GSL_{GPP} are growing season lengths based on EVI and GPP, respectively. CUP is carbon uptake period.
3. The 8-day composite EVI values were summed (EVI_{sum}) for the period of GSL_{EVI} for an individual year, then averaged for the study period.

654 Table 3. Integrated net ecosystem CO_2 exchange (NEE, g C m^{-2} $year^{-1}$), gross primary production
655 (GPP, g C m^{-2} $year^{-1}$), and evapotranspiration (ET, mm $year^{-1}$) on annual (yr) or growing season
656 (GSL) scales at the 12 grassland sites. Ecosystem water use efficiency (g C mm^{-1} ET) on annual
657 ($EWUE_{yr}$) and seasonal ($EWUE_{GSL}$) scales were derived from the ratio between annual and
658 growing season sums of GPP and ET, respectively.

Site	NEE_{yr} (± SD)	GPP_{yr} (± SD)	ET_{yr} (± SD)	$EWUE_{yr}$	NEE_{GSL} (± SD)	GPP_{GSL} (± SD)	ET_{GSL} (± SD)	$EWUE_{GSL}$
Audubon	88 ± 250	178 ± 151	264 ± 10	0.67 ± 0.55	-5 ± 110	147 ± 112	155 ± 35	0.93 ± 0.64
Flagstaff Wildfire	93	391	382	1.02	60	353	302	1.17
Kendall	-20 ± 44	188 ± 66	231 ± 37	0.79 ± 0.19	-39 ± 46	146 ± 67	138 ± 33	1.0 ± 0.3
El Reno burn	-71	1139	651	1.75	-207	1129	563	1.96 ± 0.71
El Reno control	-13	1085	714	1.52	-175	1060	603	1.74 ± 0.29
Fermi Prairie	-333	1298	660	1.97	-389	1267	580	2.23 ± 0.03
Konza	-86 ± 107	1308 ± 303	663 ± 136	1.98 ± 0.3	-186 ± 102	1206 ± 317	593 ± 132	2.03 ± 0.22
Walnut	-118	968	594	1.63	-154	938	510	1.83 ± 0.12
Brookings	-183	859	826	1.04	-181	839	742	1.19 ± 0.52
Fort Peck	9 ± 90	331 ± 178	348 ± 99	0.88 ± 0.37	19 ± 88	238 ± 148	262 ± 124	0.90 ± 0.36
Goodwin	-223 ± 204	1369 ± 261	665 ± 117	2.04 ± 0.37	-233 ± 187	1345 ± 260	636 ± 106	2.14 ± 0.4
Vaira	-55 ± 96	759 ± 204	299 ± 41	2.52 ± 0.52	-127 ± 113	751 ± 202	280 ± 34	2.65 ± 0.43

659

660 Table 4. Correlation coefficients (r) between 8-day composite values of gross primary production
661 (GPP), evapotranspiration (ET), and enhanced vegetation index (EVI) for the entire study period
662 at the 12 grassland sites.

Site	GPP~EVI	ET~EVI
Audubon	0.90	0.79
Flagstaff Wildfire	0.63	0.47
Kendall	0.85	0.72
El Reno burn	0.94	0.91
El Reno control	0.93	0.92
Fermi Prairie	0.88	0.89
Konza	0.89	0.80
Walnut	0.94	0.92
Brookings	0.73	0.81
Fort Peck	0.69	0.67
Goodwin	0.83	0.78
Vaira	0.87	0.81
Cross-sites	0.85	0.80

663

Fig. 1

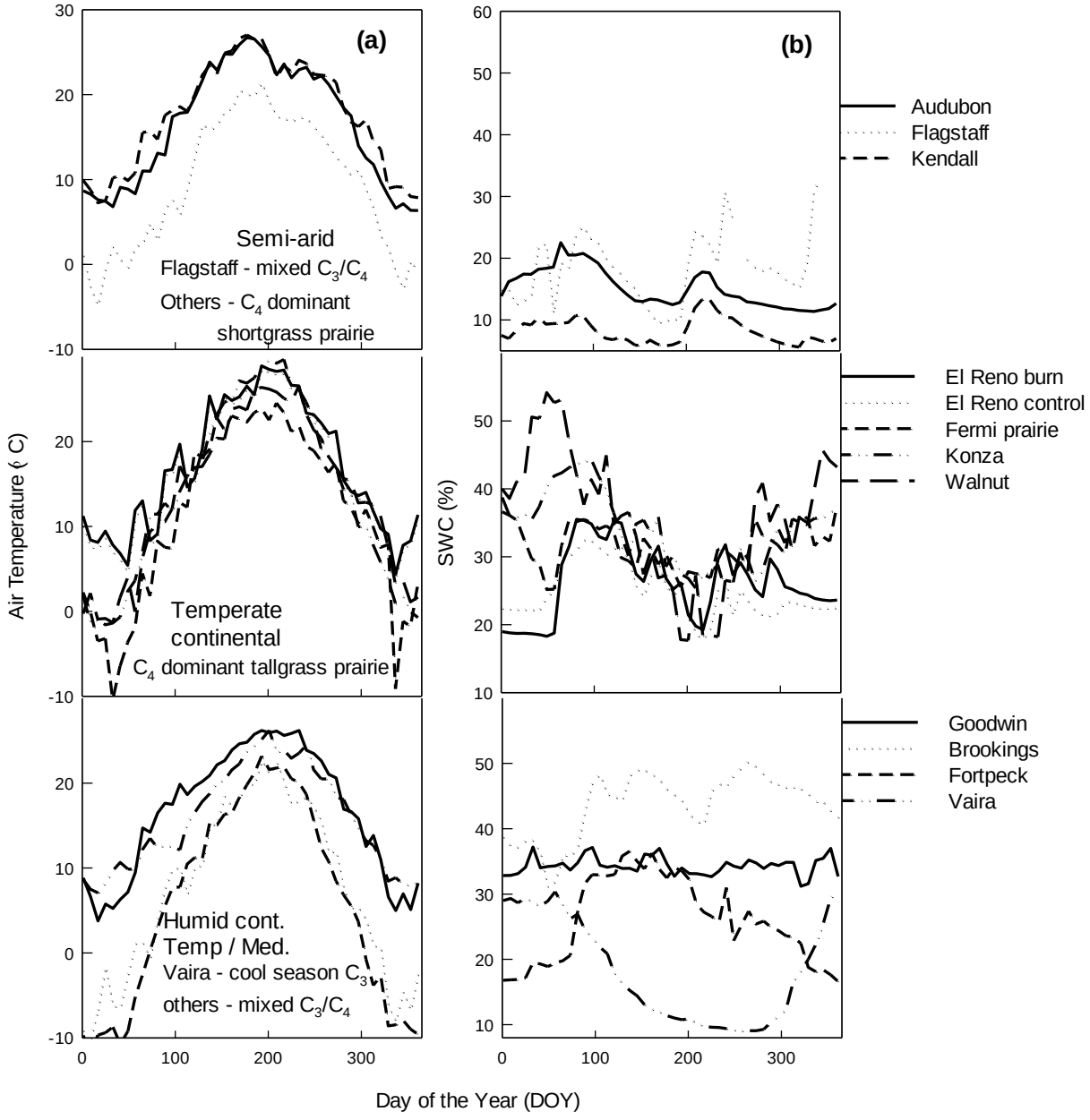
(a)
(b)
Semi-arid
Flagstaff - mixed C3/C4
Others - C4 dominant
shortgrass prairie
Temperate
continental
C4 dominant tallgrass prairie
Humid cont.
Temp / Med.
Vaira - cool season C3
others - mixed C3/C4
Air Temperature (° C)
SWC (%)
Day of the Year (DOY)
Audubon
Flagstaff
Kendall
El Reno burn
El Reno control
Fermi prairie
Konza
Walnut
Goodwin
Brookings
Fortpeck
Vaira

Fig. 2

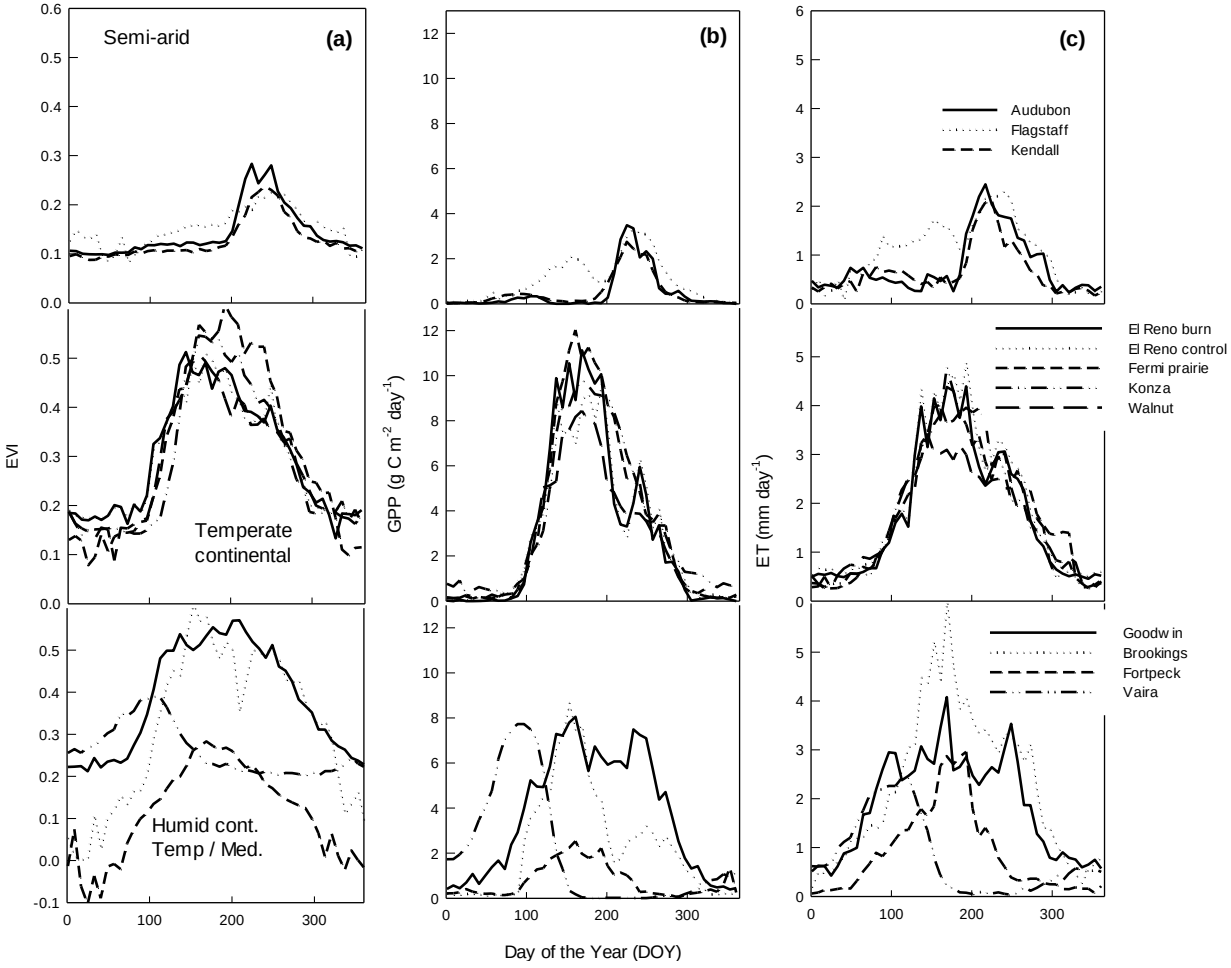
Semi-arid
(a)
Temperate continental
Humid cont. Temp / Med.
EVI
(b)
GPP (g C m-2 day-1)
(c)
ET (mm day-1)
Audubon
Flagstaff
Kendall
El Reno burn
El Reno control
Fermi prairie
Konza
Walnut
Goodwin
Brookings
Fortpeck
Vaira
Day of the Year (DOY)

Fig. 3

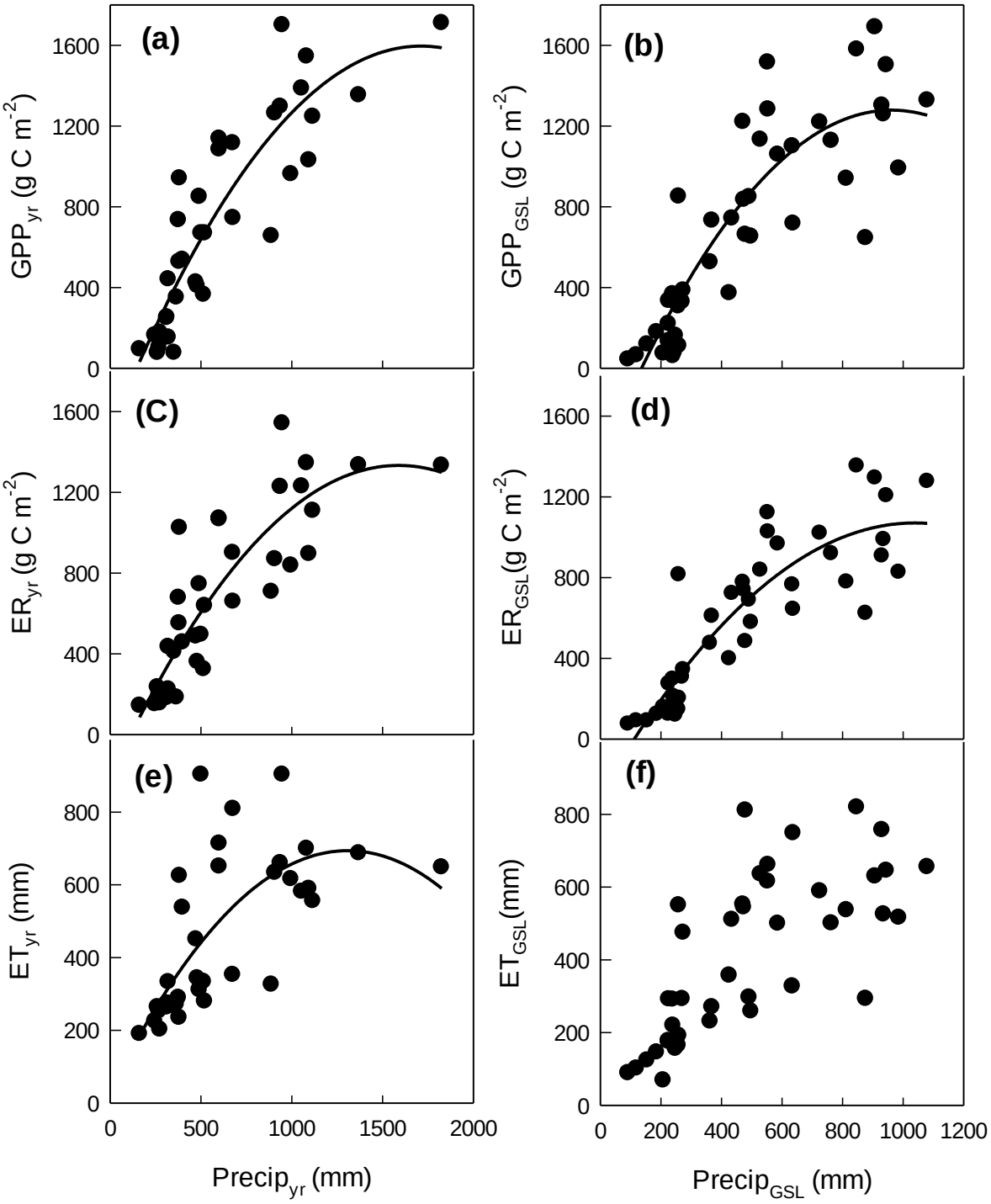
(a)
(b)
(C)
(d)
(e)
(f)
GPP$_{yr}$ (g C m^{-2})
GPP$_{GSL}$ (g C m^{-2})
ER$_{yr}$ (g C m^{-2})
ER$_{GSL}$(g C m^{-2})
ET$_{yr}$ (mm)
ET$_{GSL}$(mm)
Precip$_{yr}$ (mm)
Precip$_{GSL}$ (mm)
0
400
800
1200
1600
200
600
500
1000
1500
2000
1400

Fig. 4

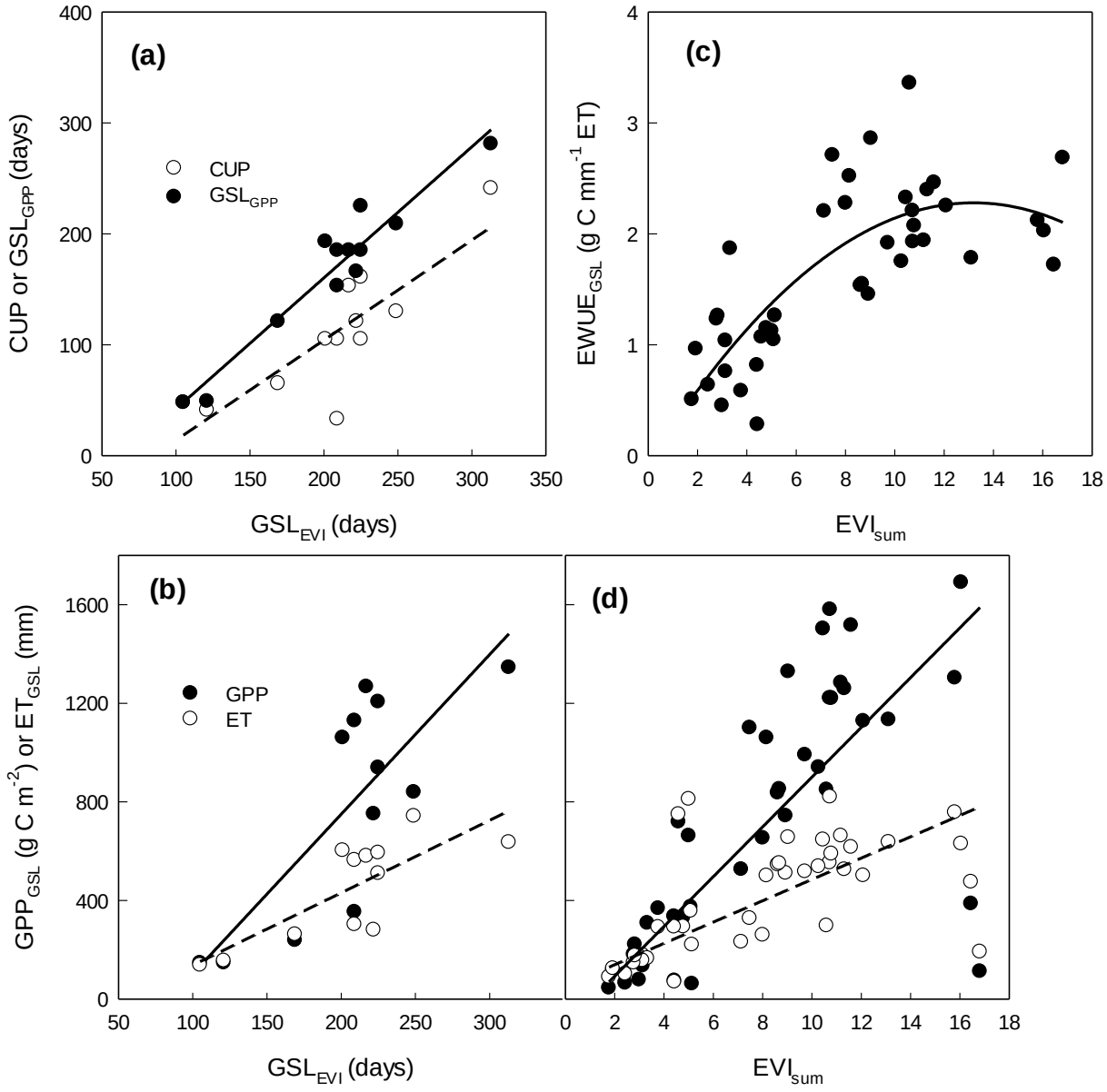
(a)
CUP
GSL$_{GPP}$
CUP or GSL$_{GPP}$ (days)
GSL$_{EVI}$ (days)
(c)
EWUE$_{GSL}$ (g C mm^{-1} ET)
EVI$_{sum}$
(b)
GPP
ET
GPP$_{GSL}$ (g C m^{-2}) or ET$_{GSL}$ (mm)
GSL$_{EVI}$ (days)
(d)
EVI$_{sum}$

Fig. 5

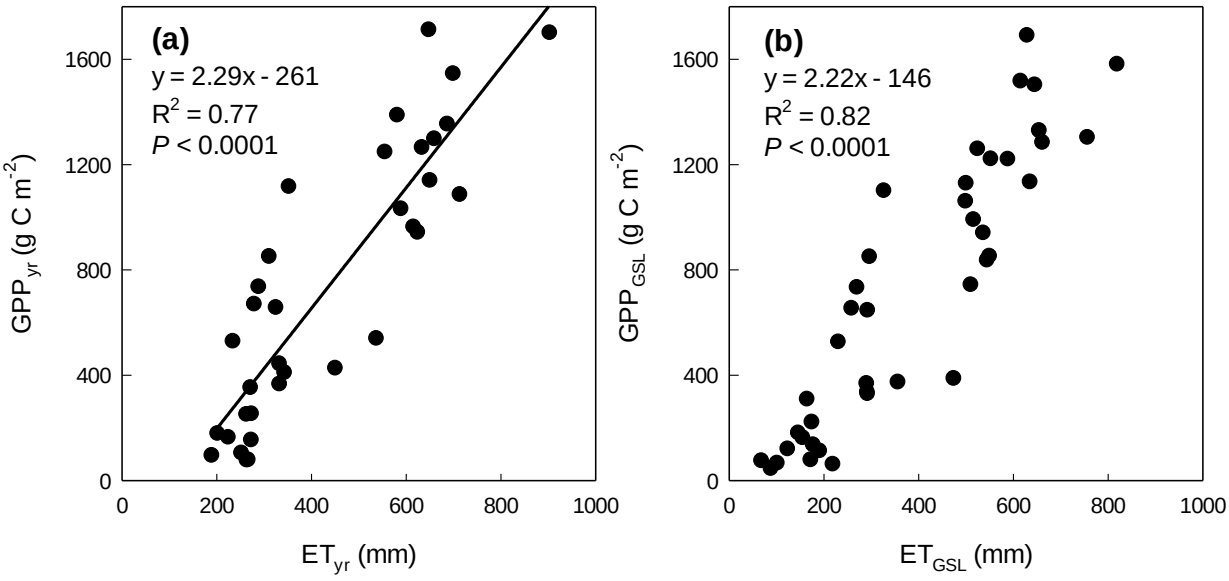
(a)
y = 2.29x - 261
R2 = 0.77
P < 0.0001
GPPyr (g C m-2)
ETyr (mm)
0
400
800
1200
1600
0
200
400
600
800
1000
(b)
y = 2.22x - 146
R2 = 0.82
P < 0.0001
GPPGSL (g C m-2)
ETGSL (mm)

Fig. 6

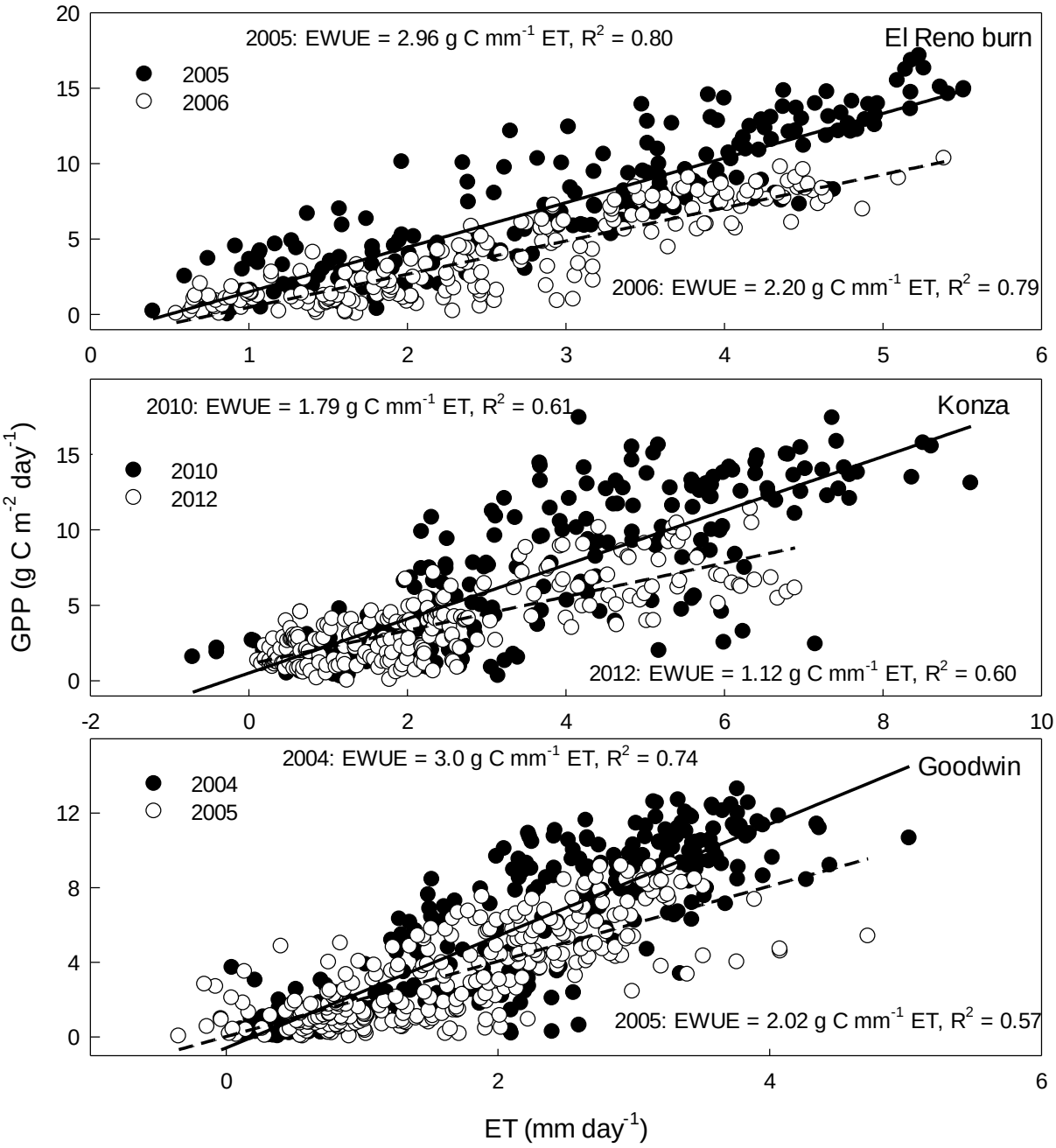
2005: EWUE = 2.96 g C mm-1 ET, R2 = 0.80
El Reno burn
2005
2006
2006: EWUE = 2.20 g C mm-1 ET, R2 = 0.79
2010: EWUE = 1.79 g C mm-1 ET, R2 = 0.61
Konza
2010
2012
2012: EWUE = 1.12 g C mm-1 ET, R2 = 0.60
2004: EWUE = 3.0 g C mm-1 ET, R2 = 0.74
Goodwin
2004
2005
2005: EWUE = 2.02 g C mm-1 ET, R2 = 0.57
GPP (g C m-2 day-1)
ET (mm day-1)

Fig. 7a

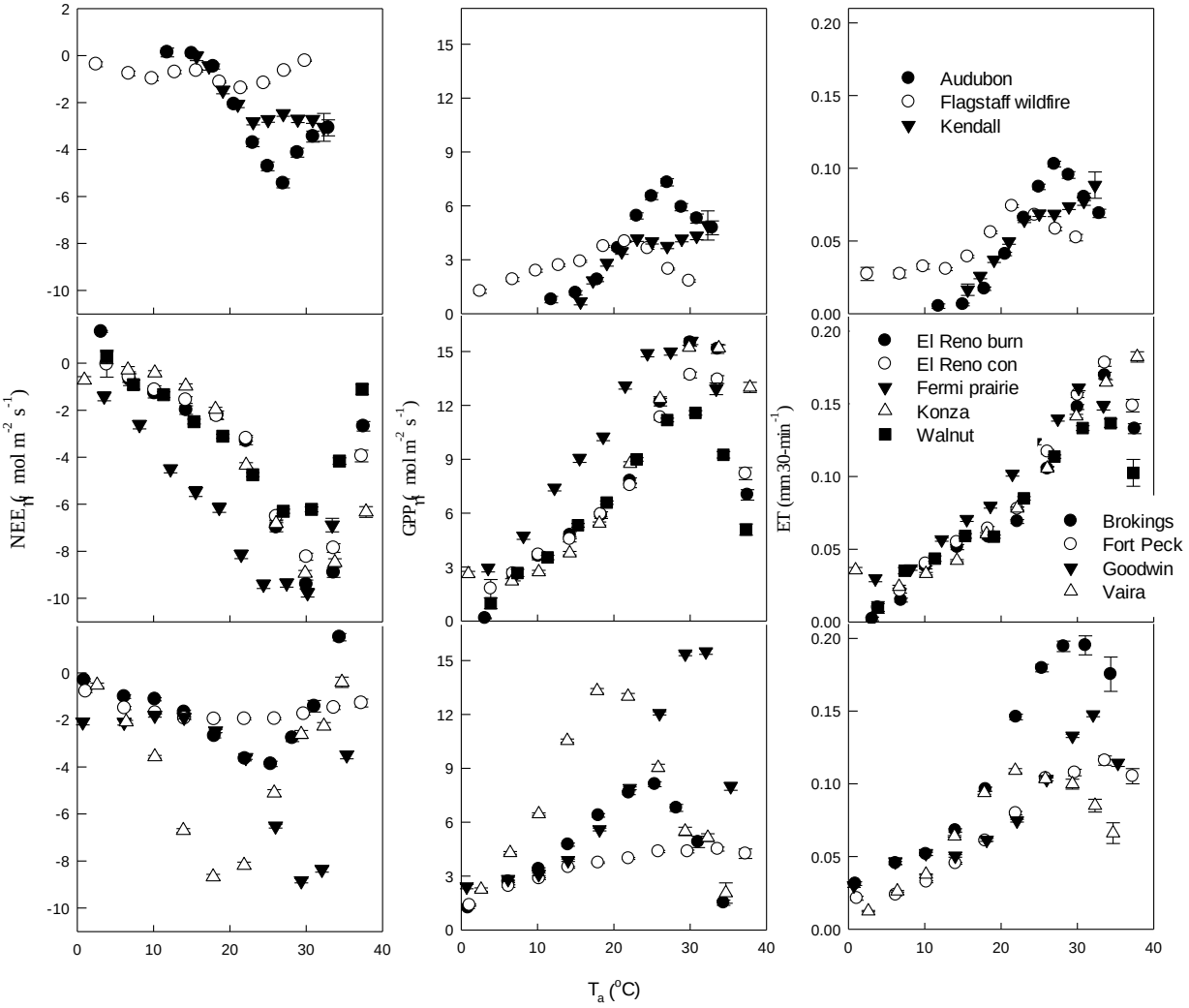
Audubon
Flagstaff wildfire
Kendall
El Reno burn
El Reno con
Fermi prairie
Konza
Walnut
Brokings
Fort Peck
Goodwin
Vaira
NEE_n (mol m^-2 s^-1)
GPP_n (mol m^-2 s^-1)
ET (mm 30-min^-1)
T_a (°C)

Fig. 7b

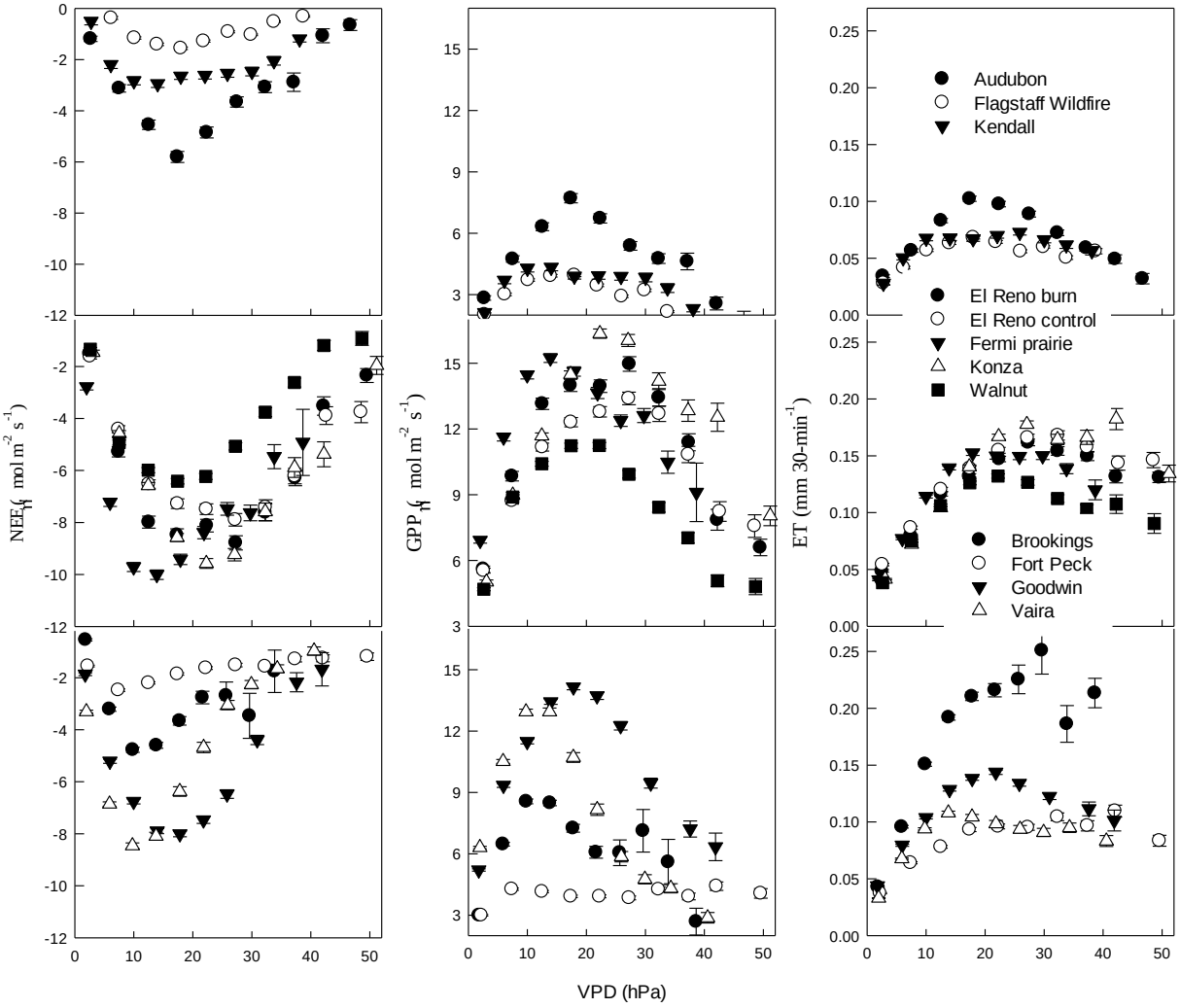
NEE (mol m-2 s-1)
GPP (mol m-2 s-1)
ET (mm 30-min-1)
VPD (hPa)
Audubon
Flagstaff Wildfire
Kendall
El Reno burn
El Reno control
Fermi prairie
Konza
Walnut
Brookings
Fort Peck
Goodwin
Vaira

Fig. 8

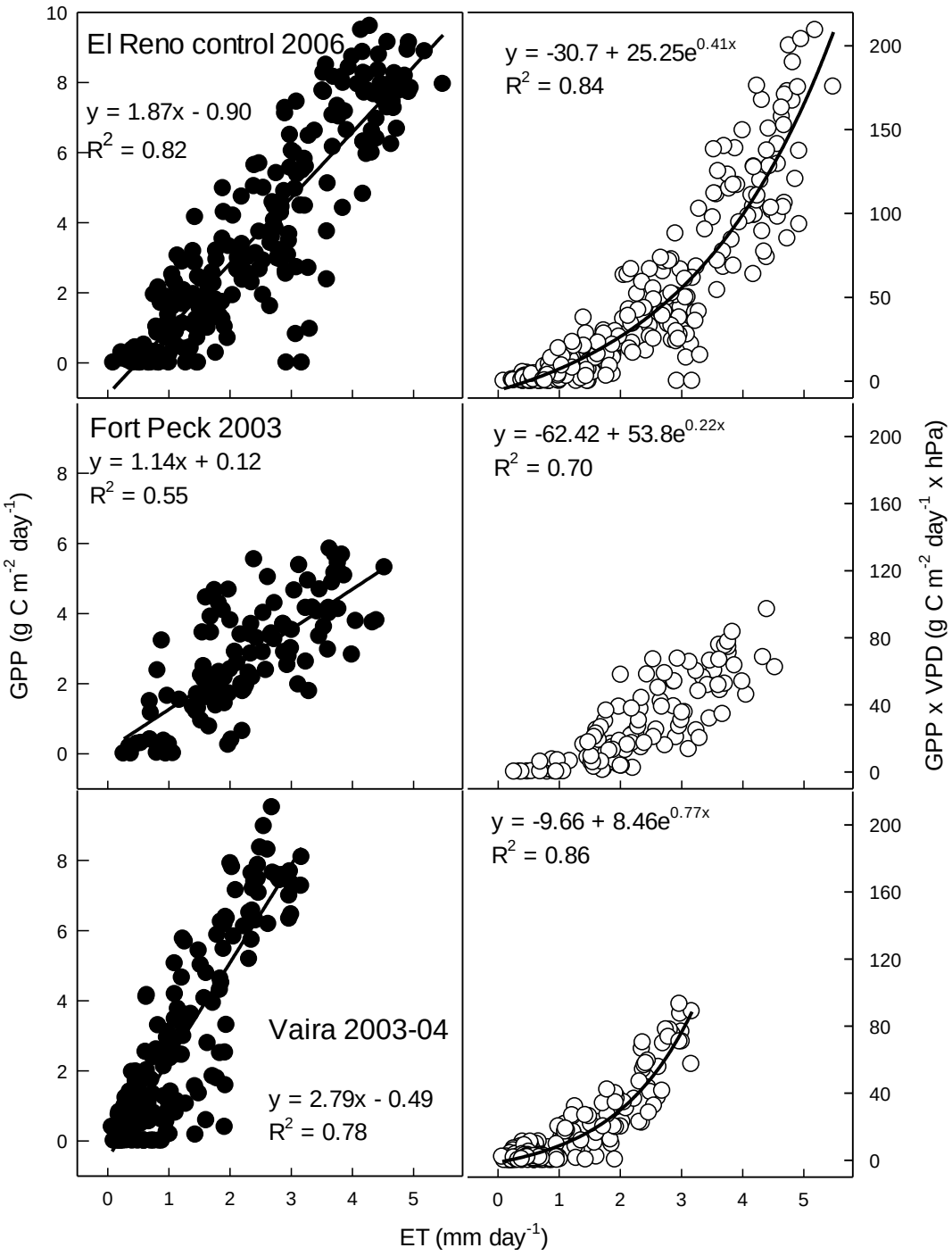
El Reno control 2006
y = 1.87x - 0.90
R2 = 0.82
y = -30.7 + 25.25e0.41x
R2 = 0.84
Fort Peck 2003
y = 1.14x + 0.12
R2 = 0.55
y = -62.42 + 53.8e0.22x
R2 = 0.70
Vaira 2003-04
y = 2.79x - 0.49
R2 = 0.78
y = -9.66 + 8.46e0.77x
R2 = 0.86
GPP (g C m-2 day-1)
GPP x VPD (g C m-2 day-1 x hPa)
ET (mm day-1)